doi:10.1016/j.jmb.2005.03.027 J. Mol. Biol. (2005) 349, 143–152

JMB

Available online at www.sciencedirect.com

SCIENCE DIRECT®

ELSEVIER

# Structural Stability of Soybean Lipoxygenase-1 in Solution as Probed by Small Angle X-ray Scattering

**Enrico Dainese[1], Annalaura Sabatucci[1], Guus van Zadelhoff[2] Clotilde Beatrice Angelucci[1], Patrice Vachette[3], Gerrit A. Veldink[2] Alessandro Finazzi Agrò[4] and Mauro Maccarrone[1]***

[1]*Department of Biomedical Sciences, University of Teramo Piazza Aldo Moro 45, 64100 Teramo, Italy*

[2]*Bijvoet Center for Biomolecular Research Department of Bio-organic Chemistry, Utrecht University Padualaan 8, 3584 CH Utrecht The Netherlands*

[3]*IBBMC, UMR 8619 CNRS Université Paris-Sud, Bât.430 91405 Orsay Cedex, France*

[4]*Department of Experimental Medicine and Biochemical Sciences, University of Rome "Tor Vergata", Via Montpellier 1, 00133 Rome, Italy*

*Corresponding author

Soybean lipoxygenase-1 (LOX-1) is used widely as a model for studying the structural and functional properties of the homologous family of lipoxygenases. The crystallographic structure revealed that LOX-1 is organized in a β-sheet N-terminal domain and a larger, mostly helical, C-terminal domain. Here, we describe the overall structural characterization of native unliganded LOX-1 in solution, using small angle X-ray scattering (SAXS). We show that the scattering pattern of the unliganded enzyme in solution does not display any significant difference compared with that calculated from the crystal structure, and that models of the overall shape of the protein calculated *ab initio* from the SAXS pattern provide a close envelope to the crystal structure. These data, demonstrating that LOX-1 has a compact structure also in solution, rule out any major motional flexibility of the LOX-1 molecule in aqueous solutions. In addition we show that eicosatetraynoic acid, an irreversible inhibitor of lipoxygenase used to mimic the effect of substrate binding, does not alter the overall conformation of LOX-1 nor its ability to bind to membranes. In contrast, the addition of glycerol (to 5%, v/v) causes an increase in the binding of the enzyme to membranes without altering its catalytic efficiency towards linoleic acid nor its SAXS pattern, suggesting that the global conformation of the enzyme is unaffected. Therefore, the compact structure determined in the crystal appears to be essentially preserved in these various solution conditions. During the preparation of this article, a paper by M. Hammel and co-workers showed instead a sharp difference between crystal and solution conformations of rabbit 15-LOX-1. The possible cause of this difference might be the presence of oligomers in the rabbit lipoxygenase preparations.



*Keywords:* calcium; catalysis; inhibitors; membranes; soybean lipoxygenase-1

## Introduction

Lipoxygenase-1 (LOX-1; linoleate:oxygen oxidoreductase; EC 1.13.11.12;) belongs to a family of non-heme, non-sulfur iron dioxygenases that take part in the metabolism of polyunsatured fatty acids, catalyzing their conversion into conjugated hydroperoxides.[1] In mammals, LOXs generate leukotrienes and lipoxins from arachidonic (eicosatetraenoic) acid,[2] and have been implicated in the pathogenesis of different inflammatory processes, such as arthritis,[3] asthma,[4–6] psoriasis,[4] brain aging[7] and human immunodeficiency virus infection.[8] In plants, LOXs favor germination and participate in the synthesis of traumatin and jasmonic acid,[9] and promote programmed cell death.[10,11] LOXs are classified after the positional specificity of arachidonic acid oxygenation into 5-, 8-, 12-, and 15-LOXs.[1] Soybean (*Glycine max* (L.) Merrill) LOX-1 is a 15-LOX, which has been used widely as a prototype for studying the functional and structural properties of the homologous family of lipoxygenases.[1,2]

Abbreviations used: SAXS, small-angle X-ray scattering; LOX, lipoxygenase; ETYA, 5,8,11,14-eicosatetraynoic acid; 13-H(P)OD, 13-hydro(pero)xy-9,11-(*E*,*Z*)-octadecadienoic acid; 9-H(P)OD, 9-hydro(pero)xy-9,11-(*E*,*Z*)-octadecadienoic acid.

E-mail address of the corresponding author: mmaccarrone@unite.it

The crystal structures of soybean LOX-1[12,13] and LOX-3.[14,15] and that of a rabbit 15-LOX-1-inhibitor complex[16] have been reported so far. In addition, three-dimensional models of the human 5-LOX have been deduced on the basis of the rabbit 15-LOX-1 crystal structure and multiple amino acid alignments.[17] Overall, these data indicate that the essential structural features of plant and animal LOXs are highly conserved, although they share only a low level of sequence homology.[1] The high-resolution structure (1.4 Å) of soybean LOX-1 (molecular mass 94 kDa) revealed that the protein is organized into two domains,[13] a β-sheet N-terminal domain (amino acid residues 1–145) and a larger, mostly helical C-terminal domain (amino acid residues 146–839). Similarly, the smaller rabbit 15-LOX-1 (molecular mass 75 kDa) comprises a C-terminal domain of about 550 amino acid residues, largely helical, and a small N-terminal domain of 111 amino acid residues, consisting of two, four-stranded antiparallel β-sheets.[16] The three-dimensional crystal structures of LOX-1 and 15-LOX-1, both 15-lipoxygenases,[1] are largely overlapping, as shown in Scheme 1. On the basis of the spatial distribution pattern of the *B*-values of the soybean LOX-1 crystal structure, it was suggested that the N-terminal domain may rock across the surface of the catalytic domain, a motion apparently compatible with the short random coil segment (amino acid residues 145–160) connecting the two domains.[13] However, both limited proteolysis experiments[18] and pH-stability studies[19] have suggested that the two domains in LOX-1 should be tightly associated, probably through ionic interactions. Here, we investigated the conformation in solution of LOX-1 using small angle X-ray scattering (SAXS), an effective method to study the low-resolution structure of proteins in solution.[20–22] We determined the conformation in solution of LOX-1 in the presence of the irreversible inhibitor eicosatetraynoic acid (ETYA),[23] which has been used to mimic the effect of substrate binding on the fluorescence spectra of the enzyme.[24] In addition, we investigated the effect of glycerol, a viscogen that modifies protein hydration,[25] on the conformation of LOX-1. The structural effects of ETYA and glycerol were correlated with their effects on catalytic efficiency and membrane-binding ability of LOX-1, two critical aspects of the biological activity of the enzyme.[1,26] All our data point towards the remarkable structural stability of soybean LOX-1, whose crystal structure is essentially preserved in solution under various conditions.

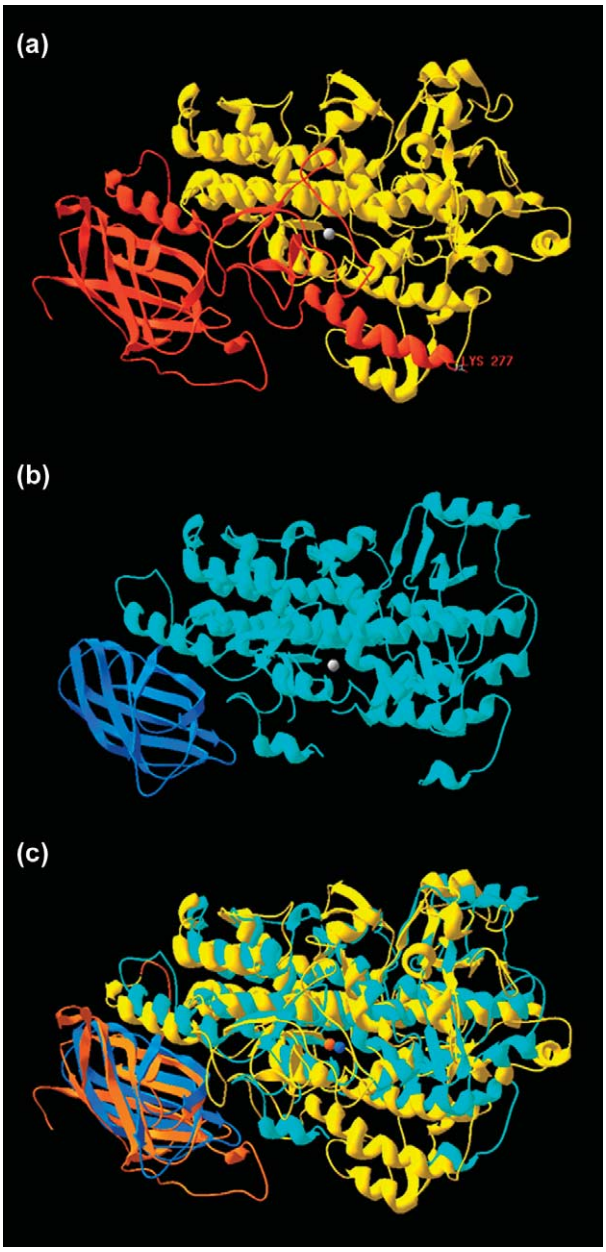


**Scheme 1.** The three-dimensional structure of soybean LOX-1 (PDB code 1yge.pdb). (a) Shown in red is the region at the N-terminal end of the polypeptide chain that is removed by digestion with trypsin; in yellow is the remaining C-terminal fragment, termed mini-LOX. The labelled lysine 277 corresponds to the trypsin cleavage site. (b) A ribbon model of rabbit 15-LOX-1 (PDB code 1lox.pdb). Shown in dark blue is the 111 amino acid residue N-terminal domain. In light blue is the C-terminal domain. (c) Superposition of the crystal structure of soybean LOX-1 (N-terminal domain and iron atom in orange; C-terminal domain in yellow) on that of rabbit 15-LOX-1 (N-terminal domain and iron atom in dark blue; C-terminal domain in light-blue). All models were drawn using the program Swiss-PdbViewer (http://www.expasy.ch/spdbv).[43] The superposition of the two structures was obtained by means of the structure alignment tool of the same software package.

## Results

### Integral parameters of soybean LOX-1 from SAXS data

Two different preparations of soybean LOX-1 were analyzed by SAXS, using buffers at different

pH and ionic strength to define the best experimental conditions under which protein–protein interparticle interactions could be minimized. In fact, a marked increase in the scattering intensity at low angles was observed even at protein concentrations of 2 mg/ml (data not shown), indicating the presence of a significant amount of soluble aggregates in solution.[27] Yet, lowering the protein concentration below 2 mg/ml by simply diluting more concentrated (7 mg/ml) stock solutions was not enough to ensure the dissociation of all aggregates, yielding SAXS patterns with a small but distinct increase of the scattering intensity at $q < 0.06$ Å$^{-1}$. In order to obtain fully monodisperse LOX-1 samples, solutions at low protein concentration (2 mg/ml) were collected by filtration through a size-exclusion HPLC column immediately before the SAXS measurements (see Materials and Methods). This HPLC separation yielded a monodisperse LOX-1 solution when eluting the column with 50 mM Tris–HCl (pH 7.0), 150 mM NaCl. However, samples obtained with the same HPLC procedure but in 50 mM sodium phosphate (pH 7.0), 150 mM NaCl, still showed the presence of a small amount of protein aggregates, suggesting that phosphate can act as a kosmotropic solute that favors the aggregation process. Finally, the LOX-1 scattering patterns obtained in Tris–HCl buffer at low (2 mg/ml) and high (7 mg/ml) protein concentration were merged, and the molecular mass of soybean LOX-1 was calculated from the zero-angle intensity (see Materials and Methods). This calculation yielded a value of 93,000($\pm$800) Da, in close agreement with the value of 94,369 Da derived from the LOX-1 primary structure.[13] This finding further confirms the monodispersity of the soybean LOX-1 solutions.

The radius of gyration of soybean LOX-1 was calculated using the Guinier approximation[28] from the range of momentum transfer ($q$), such that $qR_g < 1.3$ (Figure 1(a) and Table 1). The distance distribution function $p(r)$ was then calculated using the program GNOM,[29] and appeared to be essentially symmetric with respect to the most frequent distance, as expected for a compact particle (Figure 1(b)). The value of the maximum dimension of the particle ($D_{max}$) calculated in real space from the $p(r)$ is reported in Table 1, as well as the value of the radius of gyration, which is in good agreement with the Guinier estimate. The theoretical scattering pattern of the crystal structure of soybean LOX-1 was calculated using the program CRYSOL and atomic coordinates from the pdb file 1yge.[13] The resulting curve was in very good agreement ($\chi = 1.582$) with the experimental pattern (Figure 2), and was obtained for an electron density contrast in the solvation shell $\delta\rho_b = 33$ e/nm$^3$ (i.e. density of the solvent in the shell = 1.13 g/cm$^3$). This value is found with most soluble proteins.

**Table 1.** Comparison of the structural parameters obtained for native soybean LOX-1, alone or in the presence of 5% glycerol

| Parameter | LOX-1 | LOX-1 in 5% glycerol |
|---|---|---|
| $R_g$ (Guinier) Å | 30.0$\pm$0.5 | 30.7$\pm$0.5 |
| $R_g$ $p(r)$ Å | 29.7$\pm$0.2 | 31.0$\pm$0.2 |
| $D_{max}$ (Å) | 100$\pm$5 | 110$\pm$5 |

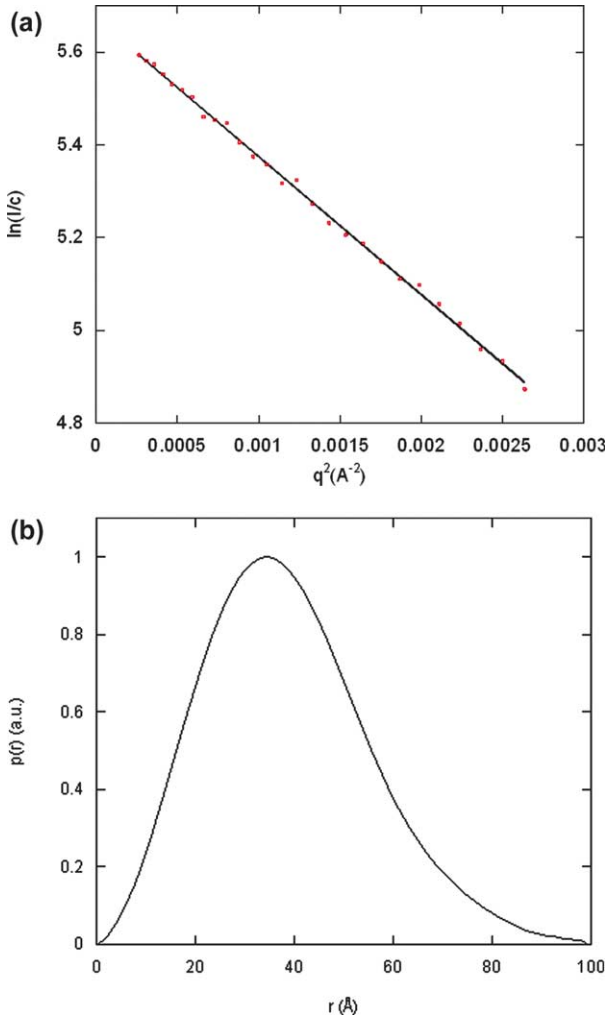


**Figure 1.** (a) A Guinier plot including the curve fit (continuous line) of soybean LOX-1 in 50 mM Tris–HCl (pH 7.0), 150 mM NaCl. (b) The $p(r)$ function of native soybean LOX-1.

## *Ab initio* models of soybean LOX-1 in solution

SAXS data were used in further analyses to obtain the overall conformation of soybean LOX-1 in solution, only after having reasonably ruled out any significant protein aggregation. *Ab initio* calculations of the shape of the molecule from the SAXS pattern were performed using the program DAMMIN.[30] Ten independent reconstructions were calculated using the program from randomly generated starting configurations (see Materials and Methods). These yielded very similar shapes, as shown by the low value of the normalized spatial

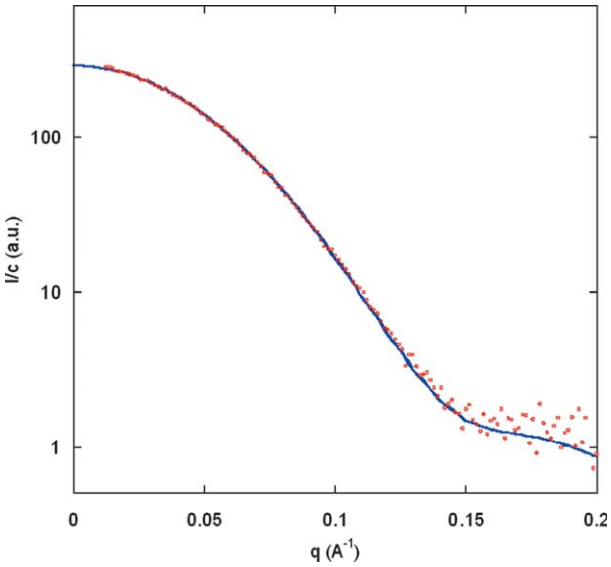


**Figure 2.** Comparison of the experimental scattering intensity of native soybean LOX-1 in solution (circles) with the pattern calculated from the atomic coordinates (PDB code 1yge.pdb) using the program CRYSOL (continuous line).

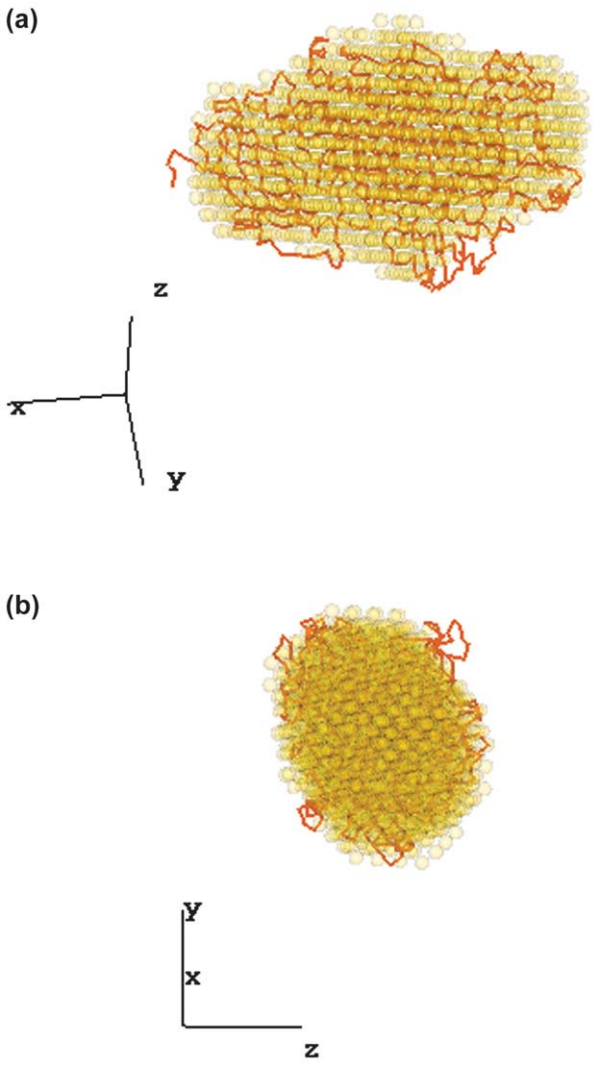


**Figure 3.** Low-resolution model obtained with the program DAMMIN for the native enzyme in solution (yellow spheres) superimposed on the crystal structure 1yge.pdb (C chain): (a) side view; (b) front view. The superimposition was performed using the program SUPCOMB (see Materials and Methods).

discrepancy (NSD) = 0.469 ± 0.016, calculated with the DAMAVER program package. The resulting DAM envelope is shown in Figure 3. The calculated pattern obtained from this final model is nearly identical with the experimental curve. Moreover, Figure 3 also shows the $C^{\alpha}$ chain of the crystal structure, superimposed on the DAM model through the program SUPCOMB. The agreement was excellent, with a value of $d = 0.923$, which indicates a very close similarity. Incidentally, this $d$ value is lower than that typically reported for the superposition of atomic structures over *ab initio* DAM models derived from solution scattering data.[31] In conclusion, our SAXS data add strong support to the view that the overall shape of LOX-1 does not undergo any significant distortion inside the crystal lattice and that in solution the N-terminal domain is associated stably with the C-terminal domain. These data are at variance with the solution structure of 15-LOX-1 from rabbit, which appeared during the preparation of this article.[32] In fact, 15-LOX-1 has been reported to exhibit a central bending between the N-terminal domain and the C-terminal domain in solution that does not show up in the crystal, suggesting a high degree of motional freedom of the N-terminal β-barrel in aqueous solutions.[32] Based on the great similarity between soybean LOX-1 and rabbit 15-LOX-1 crystal structures (Scheme 1), and on the comparable length of the interdomain linking peptide (15 residues (Ala145–Ser160) *versus* 13 residues (Gly111–Phe124), in LOX-1 and 15-LOX-1, respectively),[13,16,32] the difference in the motional freedom of the two enzymes in solution is surprising. In search of potential reasons for this difference, we analyzed the interface between the two domains for both proteins using the Protein–Protein Interaction Server.[33] The accessible surface area (*ASA*) buried within the interface appears to be significantly smaller for rabbit 15-LOX-1 (1093.32 Å$^2$) than for soybean LOX-1 (1667.23 Å$^2$). However, the values obtained for the Gap Volume Index (see Material and Methods) were the same (2.43 *versus* 2.41) and both identical with the average of 2.40 observed for interfaces between two different partners within a stable complex.[33] The interdomain interaction should therefore be quite tight in both proteins, in spite of the significantly smaller buried surface in the case of rabbit 15-LOX-1, and our data rather support the view of a tight interdomain association.[18,19]

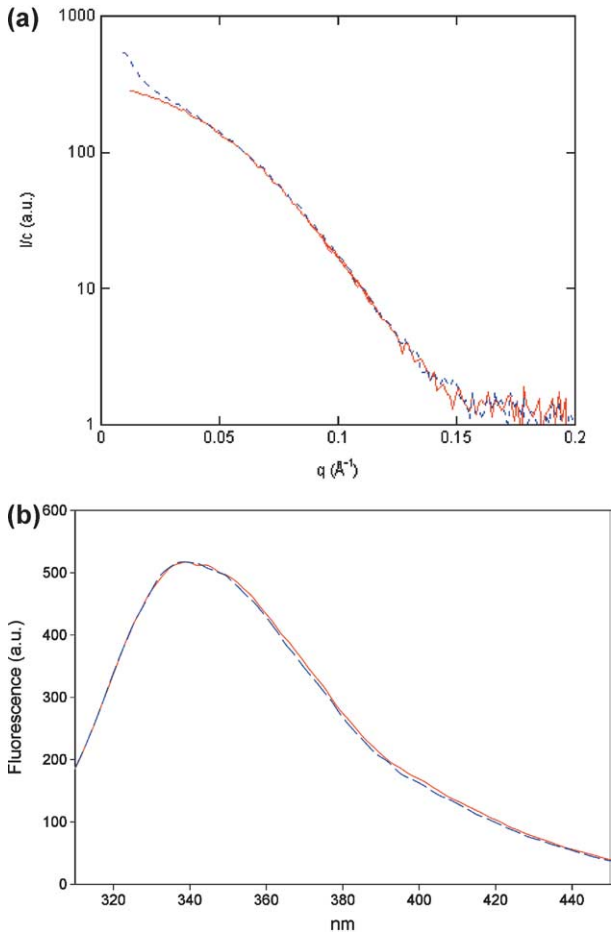


**Figure 4.** (a) Experimental X-ray scattering intensity and (b) fluorescence emission spectra of soybean LOX-1, alone (continuous line) or in the presence of a fivefold molar excess of ETYA (broken line).

## Conformation of LOX-1 in the presence of ETYA and glycerol

We next analyzed the SAXS pattern of soybean LOX-1 in the presence of a fivefold molar excess (100 μM) of ETYA, an irreversible inhibitor used to mimic substrate binding.[23,24] The SAXS pattern obtained was almost identical with that of unliganded LOX-1 at $q$ values larger than 0.04 Å$^{-1}$, yet it displayed a marked increase in intensity at lower angles (Figure 4(a)). These features are indicative of the presence of higher molecular mass soluble aggregates, the concentration of which reaches a maximum within two hours (not shown). In addition, the fluorescence spectrum of LOX-1 appears to be unaffected by the addition of a fivefold molar excess of ETYA (Figure 4(b)). Therefore, it can be concluded that ETYA does not modify the overall solution shape of LOX-1, but may promote aggregation of proteins in solution by changing the interaction potentials. Indeed, unspecific binding of ETYA outside the LOX-1 active site could favor protein–protein association, an hypothesis in keeping with previous static and dynamic fluorescence data.[24] We investigated the effect of glycerol on the conformation of LOX-1. Glycerol has long been used as a protein stabilizer,[34] and as a viscogen able to induce a preferential protein hydration.[25] In this study, we used 5% (v/v) glycerol, which increases buffer viscosity by ∼12%, and did not further increase the concentration of glycerol to avoid a significant decrease in the

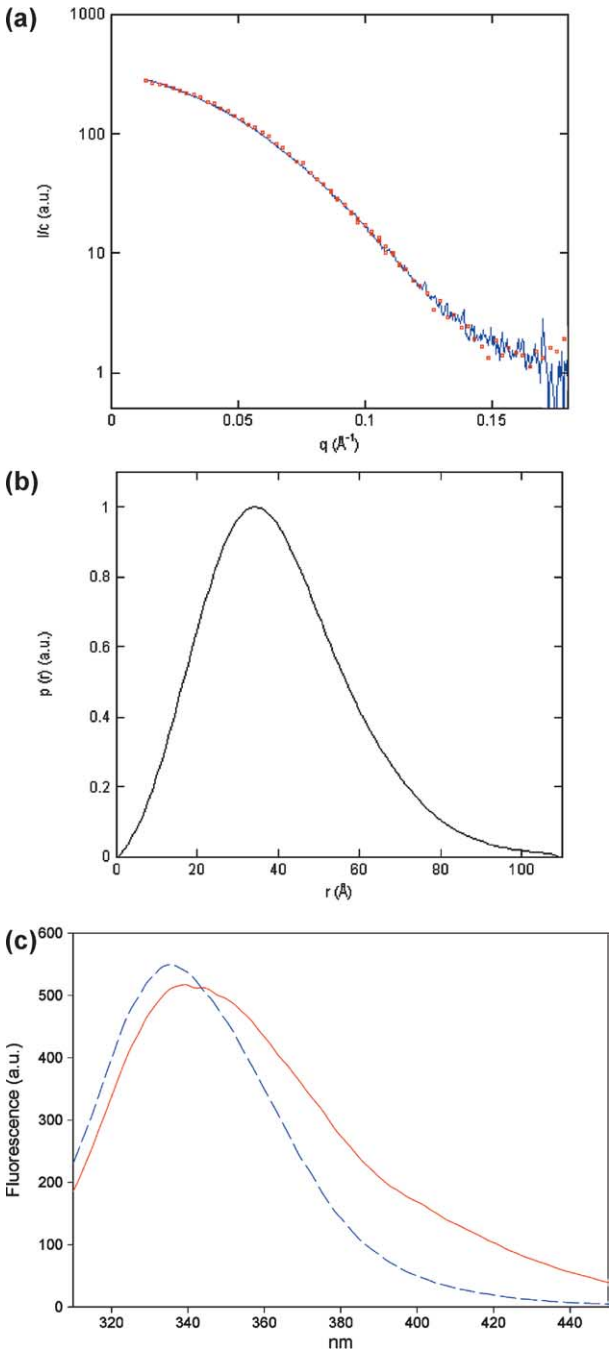


**Figure 5.** (a) Experimental X-ray scattering intensity of soybean LOX-1, alone (circles) or in the presence of 5% glycerol (continuous line). (b) The $p(r)$ of soybean LOX-1 in the presence of 5% glycerol. (c) Fluorescence emission spectra of soybean LOX-1, alone (continuous line) or in the presence of 5% glycerol (broken line).

contrast of SAXS measurements. The data obtained for LOX-1 in 50 mM Tris–HCl (pH 7.0), 150 mM NaCl, 5% glycerol, did not exhibit any upward curvature at small angles characteristic of higher molecular mass oligomers, even at concentrations of protein higher than 2 mg/ml (Figure 5(a); and data not shown). This finding suggests that glycerol stabilizes the protein in its monomeric form, and indeed the molecular mass estimate derived from the intensity at the origin (92,800($\pm$900) Da) was close to the expected molecular mass (94,369 Da) of the LOX-1 monomer.[13] The scattering pattern is very close to that of LOX-1 in the absence of glycerol, with only slightly higher values of $R_g$ and $D_{max}$ derived from the $p(r)$ analysis (see Table 1). The global conformation remains essentially unaltered in the presence of glycerol, any change being very small. In contrast, the fluorescence spectrum of soybean LOX-1 undergoes a significant blue shift ($\sim$5 nm) upon addition of glycerol (Figure 5(c)). This modification is most likely due to a change in the environment of externally exposed tryptophan residues.

### Effect of ETYA or glycerol on LOX-1 activity and membrane-binding ability

We further investigated the effect of ETYA or glycerol on the catalytic efficiency and membrane-binding ability of LOX-1, two essential aspects of the biological activity of this[1,26] as well as other lipoxygenases.[32] ETYA or glycerol were used in the same conditions (i.e. fivefold molar excess of ETYA and 5% glycerol) used to perform SAXS measurements, in order to compare the structural and functional effects of these compounds. ETYA fully and irreversibly inhibited the dioxygenation of linoleic acid catalyzed by LOX-1, extending previous findings.[23,24] Addition of glycerol (5%) had only a minor effect on the catalytic properties of the enzyme, yielding a catalytic efficiency ($k_{cat}/K_M$) value of $9.83\times10^6$ $M^{-1}$ $s^{-1}$, compared with $11.20\times10^6$ $M^{-1}$ $s^{-1}$ for the control. In addition, it yielded a small but significant ($p<0.05$) change in the regiospecificity of the dioxygenation reaction (from 100% 13-hydro(pero)xy-9,11-(*E*,*Z*)-octadecadienoic acid (H(P)OD) to 83% 13-H(P)OD and 17% 9-H(P)OD).

Soybean LOX-1 has been shown to bind negatively charged, unsaturated liposomes, and this effect has been shown to be enhanced by calcium ions.[26] Under the same experimental conditions, we found here that ETYA did not affect the membrane-binding ability of LOX-1 nor its dependence on calcium ions (Table 2), whereas the addition of glycerol (5%) increased the binding of LOX-1 to membranes significantly (up to 175% of the controls), without affecting the calcium-dependence of this process (Table 2).

## Discussion

Here, we demonstrate that the crystal structure of soybean LOX-1 is essentially preserved in solution, even after addition of ETYA or glycerol. While the effect of glycerol on LOX-1 activity extends previous data on the role of solubilizers,[35] the enhancement by glycerol of the membrane-binding ability of LOX-1 seems of interest. In fact, in a previous study we showed that tryptic digestion of soybean LOX-1 at lysine 277 removes a 30 kDa N-terminal fragment, which consists of 145 amino acid residues of the N-terminal domain plus 132 residues of the C-terminal domain (see panel (a) in Scheme 1).[26] The resulting trimmed lipoxygenase (termed mini-LOX) shows improved activity and membrane-binding ability, due to a larger hydrophobic surface[26] and a greater flexibility[24] compared with the native enzyme. The addition of glycerol seems to result in similar characteristics within the intact molecule, with no major conformational changes but through local rearrangements and relocation of side-chains at the surface of the molecule. Finally, the effects of both ETYA and glycerol seem to demonstrate that catalytic activity and membrane-binding ability of LOX-1 are not linked, and may depend on different determinants of the solution structure of the enzyme.

The stability of the crystal structure of soybean LOX-1 in solution, which remains essentially unaffected under all our experimental conditions, is remarkable and appears to be in marked contrast to the situation observed in the case of rabbit 15-LOX-1. The major discrepancies between the experimental scattering patterns in solution and the curve calculated from the atomic coordinates reported recently[32] have been interpreted in terms of a global, large movement of the N-terminal domain with respect to the C-terminal domain. This interpretation is entirely dependent on the assumption that the solution studied was monodisperse.

**Table 2.** Comparison of membrane-binding ability of native soybean LOX-1, alone or in the presence of 10 μM ETYA or 5% glycerol

| Treatment | LOX-1 | LOX-1 in ETYA | LOX-1 in glycerol |
|---|---|---|---|
| None | 0.16$\pm$0.03[a] (100) | 0.18$\pm$0.03[a] (112) | 0.28$\pm$0.02[a] (175)[b] |
| +10 μM $CaCl_2$ | 0.48$\pm$0.04 (300)[c] | 0.45$\pm$0.04 (281)[c] | 0.76$\pm$0.06 (475)[c] |
| +10 μM $CaCl_2$, +100 μM EDTA | 0.19$\pm$0.03 (100)[d] | 0.20$\pm$0.02 (125)[d] | 0.31$\pm$0.03 (194)[d] |

[a] Absorbance values at 405 nm. Values in parentheses are percentages of control (none) LOX-1.
[b] $p<0.01$ *versus* LOX-1 (none).
[c] $p<0.01$ *versus* corresponding controls (none).
[d] $p<0.01$ *versus* corresponding $CaCl_2$-treated samples ($p>0.05$ in all other cases).

This is a critical point in the study of a protein particularly prone to self-association, as explained clearly by Hammel and co-workers.[32] However, we believe that the assumption that 15-LOX-1 was indeed monodisperse is not firmly established, based on the reported protocol for sample preparation.[32] In fact, we noticed that soybean LOX-1 has a marked tendency to aggregate in solution. This phenomenon affected our first SAXS studies. We overcame this problem by modifying the buffer system appropriately and by performing a final step of purification immediately before SAXS measurements. Interestingly, the *ab initio* modeling of SAXS data from LOX-1 solutions containing small amounts of aggregates gave rise to an elongated overall shape of the protein, strikingly similar to that described by Hammel and co-workers for rabbit lipoxygenase.[32] Overall, our SAXS results in solution are compatible with the rocking movement of the N-terminal domain of LOX-1 across the surface of the C terminus, as suggested for the crystallized enzyme,[12,13] but rule out a large swing away from it.

Finally, we found that soybean LOX-1 is able to bind to membranes both in its native state and in the presence of glycerol. The latter compound determines an increase of the membrane-binding ability without affecting the overall structure of the enzyme. Taken together, these data clearly indicate that soybean LOX-1 does not require the N-terminal β-barrel domain movement proposed for the membrane binding of rabbit 15-LOX-1.[32]

## Materials and Methods

### Materials

All chemicals were of the purest analytical grade. Linoleic (9,12-octadecadienoic) acid, 5,8,11,14-eicosatetraynoic acid (ETYA), and glycerol were from Sigma Chemical Co. (St Louis, MO). Calpain from human erythrocytes, and 16S and CaeSS2 Hc from *Carcinus aestuarii* were purified as described.[36,37]

### Isolation of soybean LOX-1

Lipoxygenase-1 was purified from soybean (*G. max* (L.) Merrill, Williams) seeds as described,[38] and was then subjected to a further step of purification by fast-protein liquid chromatography (FPLC, size-exclusion column Superdex-200) using an AKTA Explorer apparatus (Pharmacia, Uppsala, Sweden). Immediately before SAXS analysis, purified LOX-1 was subjected to size-exclusion HPLC on a Waters 486 System with a Shodex Protein KW-802.5 column, in order to eliminate protein aggregates.

### Fluorescence measurements

Fluorescence emission spectra were recorded with a PerkinElmer LS50B fluorimeter (PerkinElmer Life and Analytical Sciences, Boston, MA). The excitation wavelength was 295 nm, and emission spectra were recorded between 310 nm and 450 nm in 1 cm path-length quartz cuvettes. All spectra were recorded in 50 mM Tris–HCl (pH 7.0), 150 mM NaCl, at 20 °C using 300 nM LOX-1, alone or in the presence of 1.5 μM ETYA or 5% (v/v) glycerol.

### Membrane binding and activity assay of LOX-1

The binding of LOX-1 to negatively charged, unsaturated phosphatidylcholine liposomes was performed using the liposome kit (Sigma), as described.[26] Liposome suspensions (50 μl, corresponding to 1 μmol of phosphatidylcholine) were incubated for 30 minutes at 25 °C with 2 μM LOX-1, alone or in the presence of 10 μM ETYA or 5% glycerol. In some experiments, 10 μM $CaCl_2$ or 10 μM $CaCl_2$ + 100 μM EDTA were added to the incubation mixture. The amount of LOX-1 bound to liposomes was estimated by enzyme-linked immunosorbent assay (ELISA), using specific anti-LOX-1 monoclonal antibodies (1:400), as first antibody, and goat anti-mouse alkaline phosphatase conjugate (Bio-Rad, Richmond, CA), diluted 1:1500, as second antibody.[26] Color development of the alkaline phosphatase reaction was measured at 405 nm with *p*-nitrophenyl phosphate as substrate. The ELISA test was calibrated with different amounts of LOX-1 in the presence of liposomes (1 μmol of phosphatidylcholine/well), and included wells coated with non-immune mouse serum (Nordic Immunology, Tilburg, The Netherlands) or bovine serum albumin as controls.[26] The activity of LOX-1 (2 μM) was assayed spectrophotometrically at 25 °C in 100 mM sodium borate buffer (pH 9.0), by recording the formation of conjugated hydroperoxides from linoleic acid at 234 nm.[26] The regio- and stereospecificity of LOX-1 products was analyzed by reversed phase HPLC and gas chromatography-mass spectrometry, as described.[26] Statistical analysis of the activity and binding data was performed by the non-parametric Mann–Whitney U-test, through the InStat 3 program (GraphPAD Software for Science, San Diego, CA). Biochemical data are the mean ± SD values of at least four independent determinations, each performed in duplicate.

### SAXS measurements and data analysis

SAXS experiments were carried out at the synchrotron radiation beam line D24 of LURE (Laboratoire pour l'Utilisation du Rayonnement Electromagnetique, Orsay-France). The instrument, the data acquisition system and the evacuated measuring cell have been described.[39] In the course of several measuring sessions, samples from two different preparations were used. Freshly prepared samples of LOX-1 were measured at two different concentrations in the buffer used in the final step of purification. LOX-1 solutions were circulated slowly in the measuring quartz capillary (diameter ~ 1.5 mm) to avoid any possible protein damage due to X-ray irradiation and the temperature was kept constant at 20 °C. The scattered intensities were recorded using a position-sensitive proportional detector, at a sample-detector distance allowing the range of momentum transfer $q$ from 0.01 $Å^{-1}$ to 0.23 $Å^{-1}$ ($q = 4\pi \sin\theta/\lambda$, where $2\theta$ is the scattering angle and $\lambda$ is the wavelength of the X-rays, 1.488 Å) to be covered. Eight frames of 400 seconds each were recorded. Data reduction and background subtraction were done using the program SaxsViewer (J. Pérez, unpublished). The radius of gyration ($R_g$) of the proteins in solution was determined from the lowest $q$ values of the SAXS data, using the Guinier approximation:

$$I(q) = I(0)\exp(-R_g^2 q^2/3)$$

valid over a restricted $q$-range (typically $R_g q < 1.3$).[28] The value $I(0)/c$, the scattering intensity at zero angle normalized to the protein concentration of the sample, is proportional to the molecular mass $M$ of the protein, which can be estimated after proper calibration of the intensity using reference samples. For this purpose, the following protein samples were used: native calpain from human erythrocytes (110 kDa, 1.3 mg/ml) in 50 mM sodium borate (pH 7.5) containing 0.1 mM EDTA; 16S and CaeSS2 Hc from *C. aestuarii* (450 kDa, 1.5 mg/ml and 75 kDa, 1.2 mg/ml, respectively) in 50 mM Tris–HCl (pH 7.0), 20 mM $CaCl_2$.[39]

The distance distribution function, representing the distribution of distances between any pair of volume elements within the particle, together with the structural parameters derived from $p(r)$, i.e. the maximum dimension of the particle ($D_{max}$), and the radius of gyration, were evaluated using the indirect transform method as implemented in the program GNOM.[29]

The calculation of the theoretical SAXS pattern from the atomic coordinates was obtained using the program CRYSOL,[40] that takes into account the hydration water contribution by adding a hydration layer of 3 Å thickness around the surface of the protein with an electron density contrast with bulk water $\delta\rho_b$, which is an adjustable parameter in the fit of the experimental data by the calculated curve.

The *ab initio* shape determination was performed with the dummy atom model (DAM) method,[30] using the program DAMMIN running on a Silicon Graphics® $O_2$ Workstation (Mountain View, CA). A sphere of diameter $D_{max}$ is filled by densely packed small spheres (dummy atoms) of radius $r_0 \ll D_{max}$. The DAM structure is defined by a configuration vector **X**, assigning an index to each atom corresponding to solvent (0) or solute particle (1). In keeping with the low resolution of the solution scattering data, the method starts from a random configuration and searches for a configuration $X$ minimizing $f(X) = \chi^2 + \alpha P(X)$, where $\alpha > 0$ is a positive parameter and $P(X)$ is the penalty term. Using the program package DAMAVER, ten independent *ab initio* reconstructions obtained with DAMMIN were averaged, improving the quality of shape reconstruction. The program performs the calculation of a normalized spatial discrepancy (*NSD*) among the different calculated structures, estimating the reliability of the solution. The high and low-resolution models were visualized with the graphical software package ASSA,[41] which allows three-dimensional display and manipulation of protein structures. The superposition of the PDB structures on the three-dimensional models of the protein obtained with the DAM method was performed with the program SUPCOMB 2.0.[31] The latter program allows the determination of the *NSD* parameter $d$, which is a quantitative estimate of the similarity between two different three-dimensional objects. The final value of $d$ provides a quantitative estimate of similarity between the two objects: in general, when $d < 1$, two objects of the same nature (i.e. two DAMMIN models or two atomic models) can be considered similar, while $d \geq 1.5$ is typical for the comparison between an atomic model and the corresponding DAMMIN model.[31]

### Analysis of the N-terminal and C-terminal domain interface of LOX-1

The N-terminal and C-terminal domain interfaces of soybean LOX-1 (1yge.pdb) and of rabbit 15-LOX-1 (1lox.pdb) have been analyzed using the Protein-Protein Interaction Server developed by Jones and Thornton†.[33] Among the various parameters characterizing the analyzed interface that are returned by the program, we have considered here the accessible surface area (*ASA*) and the gap index. The *ASA* is defined as the surface mapped out by the center of a probe sphere of radius 1.4 Å rolled around the van der Waals surface of the protein. For a given interface, the value is calculated for each partner in isolation and within the complex before computing the difference. The gap volume between the two interacting domains is calculated using the program SURFNET.[42] Finally, the gap index is defined as the ratio of the gap volume to the interface *ASA*. This index is a measure of the complementarity of the interacting surfaces.

## Acknowledgements

We thank the technical staff of LURE-DCI for excellent technical assistance, and Dr M. Bari and Dr R. Giacominelli Stuffler for support in the LOX assay. This work was supported by the 5th Framework Program of the European Commission "Access to Research Infrastructures" (grant no. BD 005-00), carried out at LURE, by Ministero Politiche Agricole e Forestali (grant "FORMINNOVA" 2001), by Agenzia Spaziale Italiana (grant I/R/321/02), and by Ministero dell'Istruzione, dell'Università e della Ricerca (grant "COFIN" 2003).

## Supplementary Data

Supplementary data associated with this article can be found, in the online version, at doi:10.1016/j.jmb.2005.03.027

## References

1. Brash, A. R. (1999). Lipoxygenases: occurrence, functions, catalysis, and acquisition of substrate. *J. Biol. Chem.* **274**, 23679–23682.
2. Funk, C. D. (2001). Prostaglandins and leukotrienes: advances in eicosanoid biology. *Science*, **294**, 1871–1875.
3. Inagaki, M., Tsuri, T., Jyoyama, H., Ono, T., Yamada, K., Kobayashi, M. *et al*. (2000). Novel antiarthritic agents with 1,2-isothiazolidine-1,1-dioxide (gamma-sultam) skeleton: cytokine suppressive dual inhibitors of cyclooxygenase-2 and 5-lipoxygenase. *J. Med. Chem.* **43**, 2040–2048.
4. Muller, K. (2000). Current status and recent developments in anthracenone antipsoriatics. *Curr. Pharm. Des.* **6**, 901–918.
5. Leff, A. R. (2001). Regulation of leukotrienes in the management of asthma: biology and clinical therapy. *Annu. Rev. Med.* **52**, 1–14.
6. Segraves, E. N., Shah, R. R., Segraves, N. L., Johnson, T. A., Whitman, S., Sui, J. K. *et al*. (2004). Probing the activity differences of simple and complex

† http://www.biochem.ucl.ac.uk/bsm/PP/server/

brominated aryl compounds against 15-soybean, 15-human, and 12-human lipoxygenase. *J. Med. Chem.* **47**, 4060–4065.
7. Manev, H., Uz, T., Sugaya, K. & Qu, T. (2000). Putative role of neuronal 5-lipoxygenase in an aging brain. *FASEB J.* **14**, 1464–1469.
8. Maccarrone, M., Navarra, M., Catani, V., Corasaniti, M. T., Bagetta, G. & Finazzi-Agrò, A. (2002). Cholesterol-dependent modulation of the toxicity of HIV-1 coat protein gp120 in human neuroblastoma cells. *J. Neurochem.* **82**, 1444–1452.
9. Grechkin, A. (1998). Recent developments in biochemistry of the plant lipoxygenase pathway. *Prog. Lipid Res.* **37**, 317–352.
10. Rusterucci, C., Montillet, J. L., Agnel, J. P., Battesti, C., Alonso, B., Knoll, A. *et al*. (1999). Involvement of lipoxygenase-dependent production of fatty acid hydroperoxides in the development of the hypersensitive cell death induced by cryptogein on tobacco leaves. *J. Biol. Chem.* **274**, 36446–36455.
11. Maccarrone, M., Lorenzon, T., Bari, M., Melino, G. & Finazzi-Agrò, A. (2000). Anandamide induces apoptosis in human cells *via* vanilloid receptors. Evidence for a protective role of cannabinoid receptors. *J. Biol. Chem.* **275**, 31938–31945.
12. Boyington, J. C., Gaffney, B. J. & Amzel, L. M. (1993). The three-dimensional structure of an arachidonic acid 15-lipoxygenase. *Science*, **260**, 1482–1486.
13. Minor, W., Steczko, J., Stec, B., Otwinowski, Z., Bolin, J. T., Walter, R. & Axelrod, B. (1996). Crystal structure of soybean lipoxygenase L-1 at 1.4 Å resolution. *Biochemistry*, **35**, 10687–10701.
14. Skrzypczak-Jankun, E., Bross, R. A., Carroll, R. T., Dunham, W. R. & Funk, M. O., Jr (2001). Three-dimensional structure of a purple lipoxygenase. *J. Am. Chem. Soc.* **123**, 10814–10820.
15. Skrzypczak-Jankun, E., Borbulevych, O. Y. & Jankun, J. (2004). Soybean lipoxygenase-3 in complex with 4-nitrocatechol. *Acta Crystallog. sect. D*, **60**, 613–615.
16. Gillmor, S. A., Villasenor, A., Fletterick, R., Sigal, E. & Browner, M. F. (1997). The structure of mammalian 15-lipoxygenase reveals similarity to the lipases and the determinants of substrate specificity. *Nature Struct. Biol.* **4**, 1003–1009.
17. Hemak, J., Gale, D. & Brock, T. G. (2002). Structural characterization of the catalytic domain of the human 5-lipoxygenase enzyme. *J. Mol. Model. (Online)*, **8**, 102–112.
18. Ramachandran, S., Carroll, R. T., Dunham, W. R. & Funk, M. O., Jr (1992). Limited proteolysis and active-site labeling studies of soybean lipoxygenase. *Biochemistry*, **31**, 7700–7706.
19. Sudharshan, E., Srinivasulu, S. & Appu Rao, A. G. (2000). pH-induced domain interaction and conformational transitions of lipoxygenase-1. *Biochim. Biophys. Acta*, **1480**, 13–22.
20. Svergun, D. I. & Koch, M. H. (2002). Advances in structure analysis using small-angle scattering in solution. *Curr. Opin. Struct. Biol.* **12**, 654–660.
21. Koch, M. H., Vachette, P. & Svergun, D. I. (2003). Small-angle scattering: a view on the properties, structures and structural changes of biological macromolecules in solution. *Quart. Rev. Biophys.* **36**, 147–227.
22. Zhang, W., Hirshberg, M., McLaughlin, S. H., Lazar, G. A., Grossmann, J. G., Nielsen, P. *et al*. (2004). Biochemical and structural studies of the interaction of Cdc37 with Hsp90. *J. Mol. Biol.* **340**, 891–907.
23. Ford-Hutchinson, A. W., Gresser, M. & Young, R. N. (1994). 5-Lipoxygenase. *Annu. Rev. Biochem.* **63**, 383–417.
24. Di Venere, A., Salucci, M. L., van Zadelhoff, G., Veldink, G., Mei, G., Rosato, N. *et al*. (2003). Structure-to-function relationship of mini-lipoxygenase, a 60-kDa fragment of soybean lipoxygenase-1 with lower stability but higher enzymatic activity. *J. Biol. Chem.* **278**, 18281–18288.
25. Timasheff, S. N. & Arakawa, T. (1989). Stabilization of protein structure by solvents. In *Protein Structure: A Practical Approach* (Creighton, T. E., ed.), pp. 331–345, IRL Press at Oxford University Press, Oxford, New York, Tokyo.
26. Maccarrone, M., Salucci, M. L., van Zadelhoff, G., Malatesta, F., Veldink, G., Vliegenthart, J. F. & Finazzi-Agrò, A. (2001). Tryptic digestion of soybean lipoxygenase-1 generates a 60 kDa fragment with improved activity and membrane binding ability. *Biochemistry*, **40**, 6819–6827.
27. Feigin, L. A. & Svergun, D. I. (1987). *Structure Analysis by Small Angle X-ray and Neutron Scattering*, Plenum Press, New York.
28. Guinier, A. & Fournet, G. (1955). *Small Angle Scattering of X-rays*, Wiley, New York.
29. Svergun, D. I. (1992). Determination of the regularization parameter in indirect-transform methods using perceptual criteria. *J. Appl. Crystallog.* **25**, 495–503.
30. Svergun, D. I. (1999). Restoring low resolution structure of biological macromolecules from solution scattering using simulated annealing. *Biophys. J.* **76**, 2879–2886.
31. Kozin, M. B. & Svergun, D. I. (2001). Automated matching of high- and low-resolution structural models. *J. Appl. Crystallog.* **34**, 33–41.
32. Hammel, M., Walther, M., Prassl, R. & Kuhn, H. (2004). Structural flexibility of the N-terminal beta-barrel domain of 15-lipoxygenase-1 probed by small angle X-ray scattering. Functional consequences for activity regulation and membrane binding. *J. Mol. Biol.* **343**, 917–929.
33. Jones, S. & Thornton, J. M. (1996). Principles of protein–protein interactions. *Proc. Natl Acad. Sci. USA*, **93**, 13–20.
34. Myers, J. S. & Jakoby, W. B. (1975). Glycerol as an agent eliciting small conformational changes in alcohol dehydrogenase. *J. Biol. Chem.* **250**, 3785–3789.
35. Schilstra, M. J., Veldink, G. A. & Vliegenthart, J. F. (1994). Effect of nonionic detergents on lipoxygenase catalysis. *Lipids*, **29**, 225–231.
36. Dainese, E., Minafra, R., Sabatucci, A., Vachette, P., Melloni, E. & Cozzani, I. (2002). Conformational changes of calpain from human erythrocytes in the presence of $Ca^{2+}$. *J. Biol. Chem.* **277**, 40296–40301.
37. Dainese, E., Di Muro, P., Beltramini, M., Salvato, B. & Decker, H. (1998). Subunits composition and allosteric control in *Carcinus aestuarii* hemocyanin. *Eur. J. Biochem.* **256**, 350–358.
38. Finazzi-Agrò, A., Avigliano, L., Veldink, G. A., Vliegenthart, J. F. & Boldingh, J. (1973). The influence of oxygen on the fluorescence of lipoxygenase. *Biochim. Biophys. Acta*, **326**, 462–470.
39. Dubuisson, J. M., Decamps, T. & Vachette, P. (1997). Improved signal-to-background ratio in small-angle X-ray scattering experiments with synchrotron radiation using an evacuated cell for solutions. *J. Appl. Crystallog.* **30**, 49–54.
40. Svergun, D. I., Barberato, C. & Koch, M. H. (1995).

Crysol-a program to evaluate X-ray solution scattering of biological macromolecules from atomic coordinates. *J. Appl. Crystallog.* **28**, 768–773.
41. Kozin, M. B., Volkov, V. V. & Svergun, D. I. (1997). ASSA, a program for three-dimensional rendering in solution scattering from biopolymers. *J. Appl. Crystallog.* **30**, 811–815.
42. Laskowski, R. A. (1995). SURFNET: a program for visualizing molecular surfaces, cavities, and intermolecular interactions. *J. Mol. Graph.* **13**, 323–328.
43. Guex, N. & Peitsch, M. C. (1997). SWISS-MODEL and the Swiss-PdbViewer: an environment for comparative protein modeling. *Electrophoresis*, **18**, 2714–2723.

***Edited by R. Huber***

*(Received 6 December 2004; received in revised form 7 March 2005; accepted 10 March 2005)*